OVERVIEW OF NON-LINEAR DEVICE MODELLING METHODS BASED ON VECTORIAL LARGE-SIGNAL MEASUREMENTS

Dominique Schreurs

K.U.Leuven, Div. ESAT-TELEMIC, Kardinaal Mercierlaan 94, B-3001 Heverlee, Belgium
e-mail: Dominique.Schreurs@esat.kuleuven.ac.be

ABSTRACT

Classical large-signal device models are indirectly derived from small-signal S-parameter measurements. The recent availability of full two-port vectorial large-signal measurement systems has initiated the development of new techniques to enhance the ease and accuracy of non-linear transistor modelling. In this paper, we focus to two equivalent circuit based, or "grey" box, transistor modelling methods that are based on vectorial large-signal measurements. We show that the technique of parameter optimisation is interesting to generate fast and accurate non-linear models for particular applications. The direct extraction method is preferable to determine general non-linear models, but its efficiency is strongly related to the available measurement hardware.

INTRODUCTION

Computer-aided-design of microwave circuits operating under non-linear conditions relies heavily on the quality of the large-signal models available for the active devices used. Large-signal models are mainly described by means of an electrical equivalent scheme. Since the elements of this scheme are related with the physical operation of the device, these models are also called "grey" box models. They are mostly based on vectorial small-signal, S-parameter, measurements under swept or pulsed biasing conditions. During the past years, several prototype measurement systems to characterise large-signal waveforms have been developed (1)-(4). The surplus value of having *vectorial* instead of magnitude large-signal measurements has enabled the research of non-linear modelling approaches that make direct use of vectorial large-signal measurements, in contrast to the indirect S-parameter modelling methods. In this work, we present an overview of two techniques that are applicable to grey box models.
The presented results have been obtained by the "Non-linear Network Measurement System" (NNMS) (3,5). The NNMS allows to measure both the amplitude and phase of all spectral components of the incident and scattered travelling voltage waves at the ports of a one- or two-port device-under-test (DUT). The current and voltage waveforms can easily be derived once the travelling voltage waves and the biasing parameters are known. An important feature is the possibility to excite both device ports simultaneously by different excitation signals. The frequency range of the current NNMS system is from 600 MHz to 20 GHz.
First, we describe a method based on optimisation to estimate the parameters of empirical and neural network models. Consequently, we present the procedure and the experimental validation to directly extract the state functions of a two-port device. It is important to note that, although the modelling techniques presented in this work are illustrated by only FET type microwave devices, the procedures are generally valid and can straightforwardly be extended to other microwave non-linear one- and two-port devices.

NON-LINEAR TRANSISTOR MODEL PARAMETER ESTIMATION

Microwave transistors are often represented by an equivalent circuit, which can be subdivided in an extrinsic and intrinsic part. The extrinsic part is related with the device layout and consists of linear elements. These elements can be determined by previously developed techniques and therefore we assume in this paper that the extrinsic elements have been de-embedded where necessary. Figure 1 shows the intrinsic non-linear model that is valid for FET type transistors. This model consists of four state functions, namely the parallel connection of a charge and current source at both the gate-source and drain-source ports. These state functions can be represented by look-up tables or by functional descriptions. We distinguish two functional representation types, namely empirical expressions and neural networks. Both are characterised by a number of parameters of which the values can be estimated through optimisation. Since optimisation is not suited for look-up tables, the method discussed in this Section is not applicable to look-up table models.
The classical procedure to determine these model parameters is to optimise the functions towards the DC measured state functions, e.g., I_{ds}, and/or the S-parameter measurement based state functions, e.g., C_{gs} or the corresponding large-signal Q_{gs}. A proposed extension (6) is the consistent optimisation towards all available measurements, such as DC, multi-bias S-parameter and large-signal magnitude spectral data. An obvious way to incorporate the additional phase information of vectorial large-signal measurements could be to add the measured phase of the spectral components of the terminal currents and voltages to the optimisation procedure. The drawback is that special optimisation software is required to ensure the consistency, because this method can not be implemented easily in

towards DC, S-parameter and harmonic-balance (HB) simulations.
We elaborated a non-linear model parameter estimation procedure based on only vectorial large-signal measurements (7). Since these measurements return both the amplitude and the phase of the spectral components of the voltage waves, all necessary information is contained. Therefore, we can conclude that it is sufficient to fit the model parameters towards vectorial large-signal measurements only. The advantage of our approach is that only one type of measurements, i.e., vectorial large-signal measurements, and only one type of simulation, i.e., HB analysis, are needed. We have developed this procedure on the NNMS linked to HP MDS. The advantage of the NNMS compared to Microwave Transition Analyser (MTA) based results (8,9) is the straightforward way to measure simultaneously the instantaneous currents and voltages at both device ports. The latter implies that the expressions of all the charge and current source state functions can be optimised at once.
The procedure starts by performing a number of NNMS measurements, called "experiments", where it is possible to sweep any degree of freedom, like input power, excitation frequency, DC bias, load impedance, ... but one could focus on particular experiments depending on the application. We save explicitly the excitation data in order to perform automatically the HB simulations at exactly the operating conditions at which the NNMS measurements were performed. Subsequently, the parameters of the non-linear model are estimated during one optimisation process in which all the experiments are combined. The optimisation goals are expressed in terms of minimising the difference between the measured and simulated spectral components where we consider all the significant harmonics and, if present, intermodulation products.

The presented technique can be applied to both neural networks and empirical models. As neural network, we did not define one global model, but represented each of the four device's state functions by a neural network, which can be considered as a "a priori knowledge based" pruning technique. We considered a neural network consisting of only one hidden layer with five nodes to represent I_{ds} and with three nodes for Q_{gs} and Q_{ds}. I_{gs} can be neglected for the shown experimental conditions. The independent and hence the input variables are the terminal voltages V_{gs} and V_{ds}. The functional description is of the form:

$$I_{ds}, Q_{gs}, Q_{ds} = \sum_{i=1}^{Q} \left(w_i \tanh\left(v_{i1} V_{gs} + v_{i2} V_{ds} \right) + c_i \right) \quad (1)$$

where Q is the number of nodes and where w_i, v_{i1}, v_{i2} and c_i are the parameters to be determined. The neural network accuracy can easily be increased by adding additional hidden layers and nodes, but at the cost of a lower model generation speed. To demonstrate the developed parameter estimation procedure, we have taken as empirical non-linear model, the Chalmers model for MOS transistors (10). We applied this model to a 0.18 µm x 146 µm nMOSFET (11). The device is operated in class A, while the input power is swept. All the model parameters are simultaneously optimised towards these NNMS measurements. Figure 2 compares the measured and simulated $I_{gs}(t)$ versus $V_{gs}(t)$ and the measured and simulated $I_{ds}(t)$ versus $V_{gs}(t)$ at a high input power. This Figure clearly indicates a good agreement and hence high model accuracy. The advantage of the presented approach is that realistic operating conditions easily can be included in the optimisation procedure. This is illustrated on a 0.2 µm x 100 µm lattice-matched InP HEMT (12). We applied a single-tone a_1 to the gate and a single-tone a_2 at a different fundamental frequency to the drain. Figure 3 compares the measured $I_{gs}(t)$ and $I_{ds}(t)$ with the accurately simulated results of the neural network.

The proposed parameter estimation procedure is advantageous for the often limited capability of an empirical function and small-size neural network. The choice of a particular expression or the number of hidden nodes and layers is often a compromise between simplicity and accuracy. Therefore the non-linear model often reaches the necessary accuracy only at some bias points, while the fit is worse in the other bias regions. In this case, it is difficult for the user to know which bias points should be accurately modelled for a particular large-signal application. For most applications, the class of operation (A, AB, ...) and hence the DC bias is known, but there is less knowledge about the instantaneous terminal voltages that could be reached during operation and precisely at these values the model should be accurate. Therefore we propose to perform vectorial large-signal measurements at that class of operation, such that the non-linear model can directly be optimised at the terminal voltages that are typical for that particular operating condition.

DIRECT EXTRACTION OF THE TRANSISTOR'S STATE FUNCTIONS

The complete information of vectorial large-signal measurements also allows the direct extraction of the device's state functions. This can be understood from the $I_{ds}(t)$ versus $V_{gs}(t)$ curve on Figure 2, where we recognise the typical characteristic of I_{ds} as a function of V_{gs}. The hysteresis is caused by the capacitive effects and the intrinsic delay τ. This Figure demonstrates that the contributions of non-linear charge and current sources can clearly be noticed in NNMS measurements.
In literature, several approaches to extract non-linear models from large-signal measurements have been proposed. The first notice, based on magnitude spectral measurements, was in 1989 (13). More recent methods that also include the phase information have been presented in (14,15). These methods have in common that only the most dominant

measurements at multiple bias points.

We have investigated how a complete non-linear model can directly be determined from full two-port NNMS measurements (16,17). We assume the quasi-static condition, which is valid for the frequencies used in the presented experimental validations. The incident and scattered voltage waves are measured at the extrinsic device plane. By de-embedding the extrinsic elements from the measured voltage waves, the intrinsic terminal currents I_{mi} with i=1,2 and voltages V_{gs} and V_{ds} can be calculated. I_{m1} and I_{m2} are expressed in the time domain by:

$$I_{m1}(t) = I_{gs}\left(V_{gs}(t), V_{ds}(t)\right) + \frac{dQ_{gs}\left(V_{gs}(t), V_{ds}(t)\right)}{dt} \tag{2}$$

$$I_{m2}(t) = I_{ds}\left(V_{gs}(t), V_{ds}(t)\right) + \frac{dQ_{ds}\left(V_{gs}(t), V_{ds}(t)\right)}{dt} \tag{3}$$

By defining

$$C_{11}\left(V_{gs}(t), V_{ds}(t)\right) = \frac{\partial Q_{gs}\left(V_{gs}(t), V_{ds}(t)\right)}{\partial V_{gs}} \qquad C_{12}\left(V_{gs}(t), V_{ds}(t)\right) = \frac{\partial Q_{ds}\left(V_{gs}(t), V_{ds}(t)\right)}{\partial V_{gs}}$$

$$C_{21}\left(V_{gs}(t), V_{ds}(t)\right) = \frac{\partial Q_{gs}\left(V_{gs}(t), V_{ds}(t)\right)}{\partial V_{ds}} \qquad C_{22}\left(V_{gs}(t), V_{ds}(t)\right) = \frac{\partial Q_{ds}\left(V_{gs}(t), V_{ds}(t)\right)}{\partial V_{ds}} \tag{4}$$

equations (2) and (3) can be rewritten as:

$$I_{m1}(t) = I_{gs}\left(V_{gs}(t), V_{ds}(t)\right) + C_{11}\left(V_{gs}(t), V_{ds}(t)\right)\frac{dV_{gs}(t)}{dt} + C_{12}\left(V_{gs}(t), V_{ds}(t)\right)\frac{dV_{ds}(t)}{dt} \tag{5}$$

$$I_{m2}(t) = I_{ds}\left(V_{gs}(t), V_{ds}(t)\right) + C_{21}\left(V_{gs}(t), V_{ds}(t)\right)\frac{dV_{gs}(t)}{dt} + C_{22}\left(V_{gs}(t), V_{ds}(t)\right)\frac{dV_{ds}(t)}{dt} \tag{6}$$

These are 2 equations and 6 unknowns. When only a single-tone a_1 is applied, this set of equations can be solved by performing three large-signal measurements at three different pulsations. The condition is to have three time points t_1, t_2, and t_3, where instantaneously $V_{gs}(t_1)=V_{gs}(t_2)=V_{gs}(t_3)$, $V_{ds}(t_1)=V_{ds}(t_2)=V_{ds}(t_3)$, $\frac{dV_{gs}(t_1)}{dt} \neq \frac{dV_{gs}(t_2)}{dt} \neq \frac{dV_{gs}(t_3)}{dt}$ and $\frac{dV_{ds}(t_1)}{dt} \neq \frac{dV_{ds}(t_2)}{dt} \neq \frac{dV_{ds}(t_3)}{dt}$.

In the particular case where only the current state functions are extracted, every (V_{gs},V_{ds}) needs only to be covered by one large-signal measurement, according to the recently proposed method (18). The principle is to apply a complex load, such that the $V_{ds}(t)$ waveform versus the $V_{gs}(t)$ waveform becomes a single-valued function. The advantage is that both measurement and calculation time decrease compared to the general case where all state functions are extracted simultaneously.

The need for three independent measurements increases significantly the minimum number of NNMS measurements necessary to generate a complete non-linear model. This minimum number can be optimised by exploiting all the degrees of freedom in the NNMS set-up to reach an excellent coverage of the state variable plane (V_{gs},V_{ds}) within one large-signal measurement. The advantage of the NNMS compared to the MTA is that RF signals can be simultaneously injected at both ports 1 and 2. These are important additional degrees of freedom, because not only the amplitude of the two incident signals can be varied, but also their phase difference and their respective frequencies. The importance of a good choice of the degrees of freedom is illustrated on Figures 4 and 5. A 0.2 µm x 100 µm lattice-matched InP HEMT (12) is excited by a single-tone a_1 at the gate and by a single-tone a_2 at a different fundamental frequency at the drain. Figure 4 shows how the (V_{gs},V_{ds}) plane can be covered by two NNMS measurements with well-chosen DC biases. We defined a rectangular grid on the (V_{gs},V_{ds}) plane and investigated how many of these grid points are at least three times covered as a function of excitation signal conditions and the number of NNMS measurements (Figure 5). In case 1, the DC bias condition has been kept fixed and only the phase of a_2 has been varied. We notice on Figure 5 that the surplus information when performing more than 15 NNMS measurements is minor. In case 2, we consider the two DC bias conditions in combination with an a_2 phase variation. For the same number of NNMS measurements, more grid points are covered compared to case 1. The reason is that, although the phase of a_2 can be varied, it is not possible to cover a complete rectangular grid due to the physical inverter characteristic of the HEMT. Therefore, a better coverage can be obtained by selecting appropriate DC bias conditions. In case 3, we applied the case 2 conditions at two different fundamental frequencies of a_1. Figure 5 shows that under these conditions, about 120 (V_{gs},V_{ds}) grid points can be covered at least three times by 30 NNMS measurements. The difference with case 2 is the larger variation in V_{gs} and V_{ds} time derivatives' values when performing NNMS measurements at different fundamental frequencies, which implies that the solvability conditions are easier met. This example gives an impression of the possible reduction of the minimum number of necessary measurements when performing NNMS measurements instead of the classical DC and vectorial linear measurements.

e.g., the NNMS bandwidth and the availability of an RF multi-sine source. A reason is that in order to maximise the number of (V_{gs},V_{ds}) points covered by one NNMS measurement, the frequency shift between a_1 and a_2 should be small and the input powers of both a_1 and a_2 should be large. The latter involves a high number of non-negligible harmonics and intermodulation products to be measured. Furthermore, the actual number of grid points at which the state functions can be calculated is also related with the required extraction accuracy. Since there are several orders of magnitude difference between the elements to be extracted (device currents are typical in the mA range, while device capacitors are typical in the fF range), the solvability of the set of equations (5) and (6), expressed by a condition number, requires that the three V_{gs} and three V_{ds} time derivatives have to be significantly distinct. Consequently, the extraction algorithm needs to be an iterative procedure, where additional measurements are taken as long as at a certain (V_{gs},V_{ds}) grid point the condition number is not smaller than a predefined value (19). The measurement capabilities are here also important, as e.g., high fundamental frequencies lead to a clearer distinction of the capacitive effects. The conclusion is that the minimum number of necessary vectorial large-signal measurements for an accurate non-linear model extraction is not a priori significantly less compared to the minimum number of necessary S-parameter measurements in the adaptive Root model (20).
We applied this extraction procedure to a 0.18 µm x 146 µm nMOSFET (11). Figure 6 presents the extracted I_{ds} and C_{11}, which are the two most important non-linear elements, as a function of V_{gs} and at V_{ds} equal to 0.8 V. The accuracy of these NNMS based extractions can be determined by comparing them to the results obtained by standard DC and S-parameter measurements on the same device. Figure 6 shows a good agreement, which validates the basic principle of the developed NNMS measurement based non-linear extraction procedure.

COMPARISON OF GREY BOX NON-LINEAR MODELLING METHODS

There exist three main methods to determine the grey box non-linear model of microwave devices. The most common method is to derive the non-linear model from multi-bias S-parameter measurements. Methods based on vectorial large-signal measurements are parameter optimisation and direct extraction. Table 1 summarises the comparison between these three techniques. The advantage of the two NNMS based methods is that non-linear models are determined straightforwardly from large-signal measurements and that hence no detour via vectorial small-signal measurements is necessary. Secondly, the required device knowledge is less, because the number of state variables can be estimated from the NNMS measurements. Furthermore, the covered bias range can be extended, since extreme bias conditions are only reached temporarily by the vectorial large-signal measurements. Finally, less measurements are necessary to deduce the model than would be needed to determine a non-linear model from small-signal measurement data. In case of the direct extraction method, this reduction is strongly related to the ranges of the degrees of freedom of the measurement system. We would suggest to use the parameter optimisation method in case the envisaged application is known, such that the DUT can appropriately be excited, and to use the direct extraction method in case the goal is to obtain a general model.

CONCLUSIONS

Accurate non-linear models directly based upon vectorial large-signal measurements are perfectly possible with the NNMS measurement technology. We have explained two recent modelling approaches. First, we have discussed the straightforward parameter optimisation method that is applicable to empirical and neural network models. Secondly, we have shown that the complete non-linear quasi-static model of a two-port device can directly be extracted. The conclusion of this overview is that vectorial large-signal measurements can deliver substantial information to improve non-linear transistor models and hence circuit design. Consequently, less design iterations will be necessary, which will result in a significant reduction of development time.

ACKNOWLEDGEMENTS

The author acknowledges Hewlett-Packard for the donation of the Non-linear Network Measurement System and the IMEC MCP/NMC and STDI/CMOS groups for providing the devices. This paper presents research results of the Belgian program on interuniversity attraction poles (IUAP-IV/2). D. Schreurs is supported by the Fund for Scientific Research-Vlaanderen as a post-doctoral researcher.

REFERENCES

(1) F. van Raay and G. Kompa, "A new on-wafer large-signal waveform measurement system with 40 GHz harmonic bandwidth", 1992, IEEE MTT-S Int. Microwave Symp. Digest, pp. 1435-1438.
(2) M. Demmler *et al.*, "A vector corrected high power on-wafer measurement system with a frequency range for the higher harmonics up to 40 GHz", 1994, Proc. 24th European Microwave Conference, pp. 1367-1372.
(3) J. Verspecht *et al.*, "Accurate on wafer measurement of phase and amplitude of the spectral components of incident and scattered voltage waves at the signal ports of a nonlinear microwave device", 1995, IEEE MTT-S Int. Microwave Symp. Digest, pp. 1029-1032.

MTT-S Int. Microwave Symp. Digest, pp. 1239-1242.
(5) J. Verspecht, "Calibration of a measurement system for high frequency nonlinear devices", 1995, PhD thesis, Vrije Universiteit Brussel.
(6) J. Bandler *et al.*, "Efficient large-signal FET parameter extraction using harmonics", 1989, IEEE Trans. Microwave Theory Techn., pp. 2099-2108.
(7) D. Schreurs *et al.*, "Easy and accurate empirical transistor model parameter estimation from vectorial large-signal measurements", 1999, IEEE Int. Microwave Symp. Digest, pp. 753-756.
(8) U. Lott, "Ersatzschaltung eines GaAs MESFET gewonnen aus Messungen von Betrag und Phase der in ihm erzeugten Harmonischen", 1990, PhD thesis, E.T.H. Zürich.
(9) J. Leckey *et al.*, "Nonlinear MESFET parameter estimation using harmonic amplitude and phase measurements", 1994, IEEE MTT-S Int. Microwave Symp. Digest, pp. 1563-1566.
(10) L. Bengtsson *et al.*, "An empirical high-frequency large-signal model for high-voltage LDMOS transistors", 1998, Proc. 28th European Microwave Conference, pp. 733-738.
(11) Badenes *et al.*, "A high performance 0.18 μm CMOS technology designed for manufacturability", 1997, Proc. 27th European Solid-State Device Research Conference, pp. 404-407.
(12) K. van der Zanden *et al.*, "W-band high-gain amplifier using InP dual-gate HEMT technology", 1997, Proc. 9th Int. Conf. on Indium Phosphide and Related Materials, pp. 249-252.
(13) S. Maas and A. Crosmun, "Modeling the gate I/V characteristic of a GaAs MESFET for volterra-series analysis", 1989, IEEE Trans. Microwave Theory Techn., pp. 1134-1136.
(14) A. Werthof *et al.*, "Direct nonlinear FET parameter extraction using large-signal waveform measurements", 1993, IEEE Microwave and Guided Wave Letters, pp. 130-132.
(15) M. Demmler *et al.*, "Direct extraction of non-linear intrinsic transistor behaviour from large signal waveform measurement data", 1996, Proc. 26th European Microwave Conference, pp. 256-259.
(16) D. Schreurs *et al.*, "Direct extraction of the non-linear model for two-port devices from vectorial non-linear network analyzer measurements", 1997, Proc. 27th European Microwave Conference, pp. 921-926.
(17) D. Schreurs, "Measurement based modelling of heterojunction field-effect devices for non-linear microwave circuit design", 1997, PhD thesis, K.U.Leuven.
(18) M. Curras-Francos *et al.*, "Direct extraction of nonlinear FET I-V functions from time domain large signal measurements", 1998, Electronics Letters, pp. 1993-1994.
(19) D. Schreurs, "Non-linear device modelling and circuit design based on vectorial large-signal measurements", 1998, Int. Workshop on Integrated Nonlinear Microwave and Millimeterwave Circuits, pp. 28-42.
(20) D. Root *et al.*, "Technology independent large signal non quasi-static FET models by direct construction from automatically characterized device data", 1991, Proc. 21th European Microwave Conference, pp. 927-932.

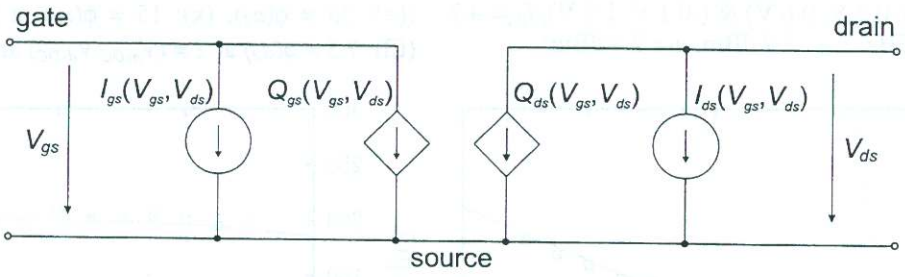

Figure 1: Intrinsic quasi-static non-linear FET model.

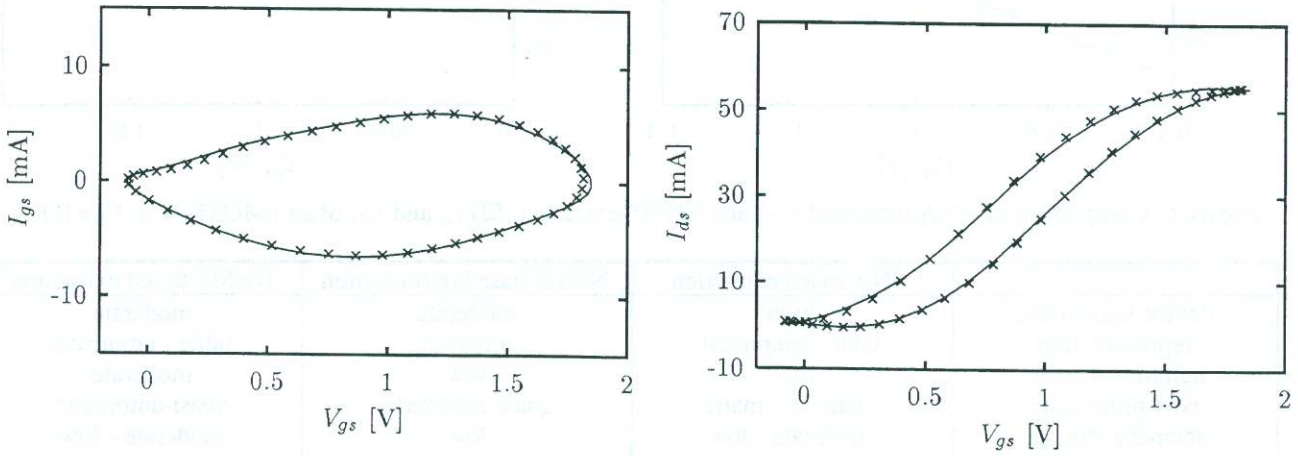

Figure 2: Measured (x) and simulated (—) $I_{gs}(t)$ versus $V_{gs}(t)$ and $I_{ds}(t)$ versus $V_{gs}(t)$ of an nMOSFET (V_{gsDC}= 0.9 V, V_{dsDC}= 1.8 V, f_0= 3.6 GHz, P_{in}= 3.8 dBm).

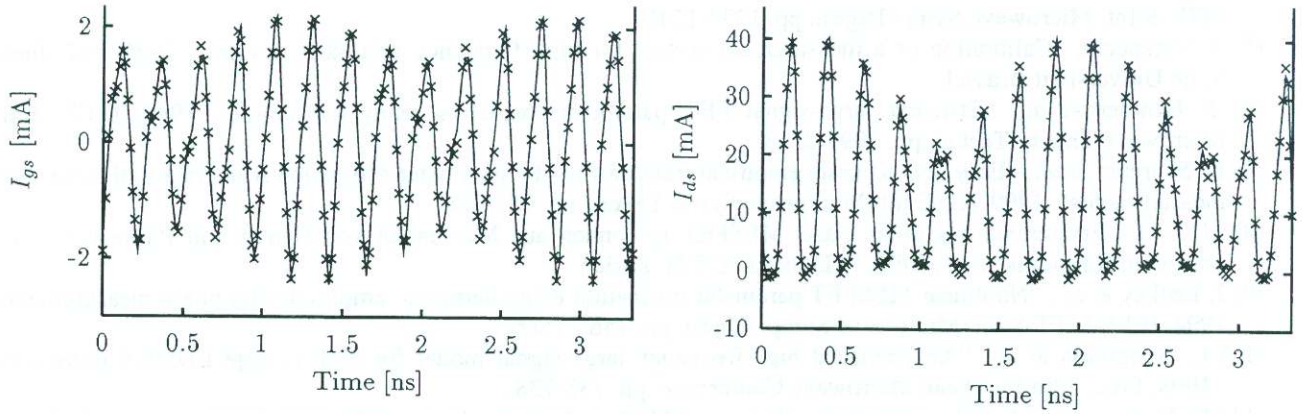

Figure 3: Comparison of the measured (x) and neural network based simulated (—) $I_{gs}(t)$ and $I_{ds}(t)$ waveforms of an InP LM HEMT excited by a two-tone signal (V_{gsDC}= -0.1 V, V_{dsDC}= 1.2 V, $f_{0,1}$= 4.2 GHz, $f_{0,2}$= 4.8 GHz, a_1= -3.9 dBm, a_2= 2.4 dBm, $\phi(a_2)$-$\phi(a_1)$= -95°).

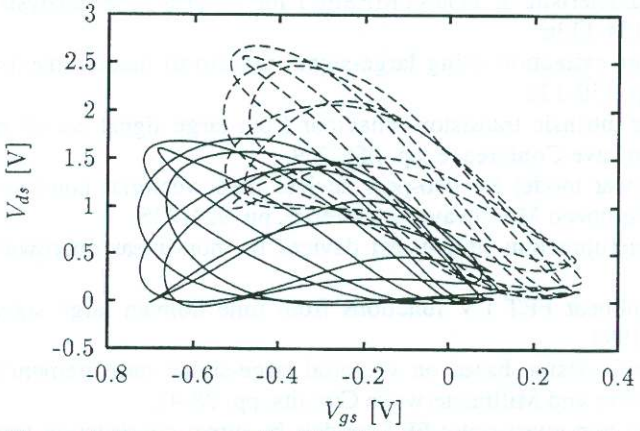

Figure 4: Coverage of the (V_{gs},V_{ds}) plane by two NNMS measurements at two DC biases on an InP LM HEMT ((V_{gsDC},V_{dsDC})= (-0.3 V, 0.6 V) & (-0.1 V, 1.2 V), $f_{0,1}$= 4.2 GHz, $f_{0,2}$= 4.8 GHz, a_1= -3.9 dBm, a_2= 2.4 dBm).

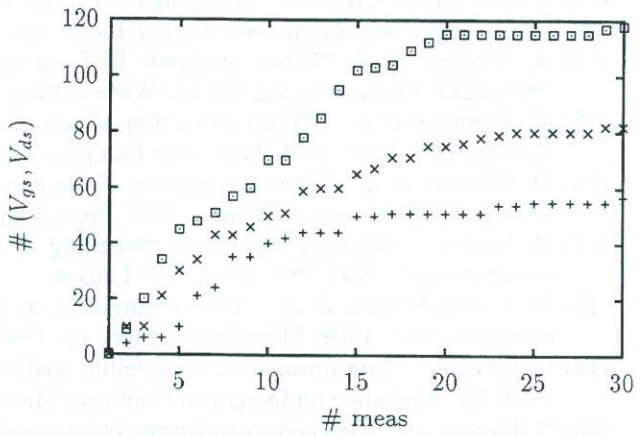

Figure 5: Number of covered (V_{gs},V_{ds}) grid points versus number of NNMS measurements on an InP LM HEMT ((+): 30 ≠ $\phi(a_2)$, (x): 15 ≠ $\phi(a_2)$ at 2 ≠ (V_{gsDC},V_{dsDC}), (□): 7.5 ≠ $\phi(a_2)$ at 2 ≠ (V_{gsDC},V_{dsDC}) and at 2 ≠ $f_{0,1}$).

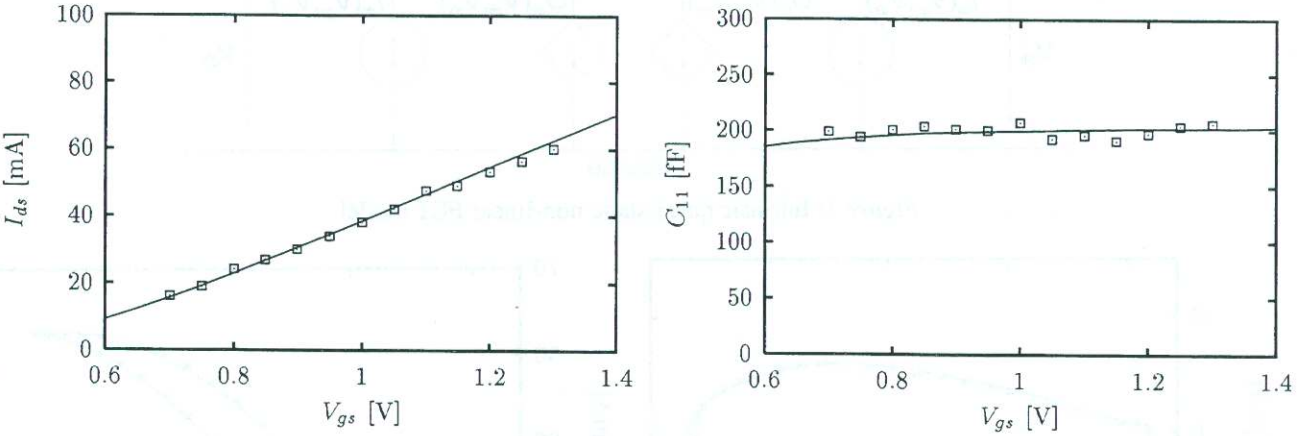

Figure 6: Comparison of VNA measured (—) and NNMS extracted (□) I_{ds} and C_{11} of an nMOSFET at V_{ds}= 0.8 V.

	VNA based extraction	NNMS based optimisation	NNMS based extraction
device knowledge	high	moderate	moderate
representation	table - empirical	empirical	table - empirical
number of meas.	high	low	moderate
post-processing	quasi-automatic	quasi-automatic	quasi-automatic
memory storage	moderate - low	low	moderate - low
validity range	limited extrapolation	limited extrapolation	limited extrapolation

Table 1: Comparison of grey box non-linear modelling techniques.